INFILTRATION OF WATER INTO SOIL WITH CRACKS

By V. Novák,[1] J. Šimůnek,[2] and M. Th. van Genuchten[3]

ABSTRACT: This paper presents the physical basis of the FRACTURE submodel for simulating infiltration of precipitation/irrigation water into relatively dry, cracked, fine-textured soils. The FRACTURE submodel forms part of the HYDRUS-ET variably saturated flow/transport model. Infiltration into the soil matrix is formally divided into two components: (1) Vertical infiltration through the soil surface; and (2) lateral infiltration via soil cracks. The first component is described and solved using the 1D Richards' equation. Excess water that does not infiltrate through the soil surface is either considered to be runoff, if no soil cracks are present, or routed into soil cracks from where it may laterally infiltrate into the soil matrix. Horizontal infiltration from soil cracks into the soil matrix is calculated using the Green-Ampt approach and incorporated as a positive source/sink term S_f in the Richards' equation describing flow in the matrix. In addition to the hydraulic properties of the soil matrix, the FRACTURE submodel requires parameters characterizing the soil cracks, notably the specific crack length per surface area l_c and the relationship between crack porosity P_c and the gravimetric soil water content w. An example problem shows that infiltration from soil cracks can be an important process affecting the soil water regime of cracked soils. A comparison with the more traditional approach, involving surface infiltration only, indicates important differences in the soil water content distribution during a rainfall/irrigation event. This extension of the classical approach to include crack infiltration significantly improves the identification and prediction of the soil water regime.

INTRODUCTION

Soils often exhibit a variety of heterogeneities such as fractures, fissures, cracks, macropores of biotic origin, and interaggregate pores (Gerke and van Genuchten 1993a; Jarvis 1998). These heterogeneities can significantly affect water and solute movement in soils by creating nonuniform velocity fields with spatially variable flows. The resulting nonuniform flow process is often referred to as preferential flow. Preferential flow may be particularly significant in fine-textured, shrinking/swelling soils containing cracks. Infiltration of precipitation and/or irrigation water into such low-permeable soils is normally very slow and frequently accompanied with surface runoff. The presence of drying cracks often decreases the amount of surface runoff by increasing the total infiltration rates and, concomitantly, the soil water content in deeper parts of the soil profile. Hence, cracks greatly affect the irrigation efficiency, as well as minimize the amount of irrigation water lost to surface runoff. At the same time crack infiltration is also associated with accelerated solute transport, with surface-applied solutes generally penetrating much deeper into the soil profile, thus posing risks for soil and ground-water pollution, including nutrients moving quickly below the root zone of agricultural crops.

Adequate descriptions of nonuniform water infiltration into initially dry, cracked, fine-textured soils are lacking in most soil-water-plant-atmosphere models. Ignoring the infiltration of water via soil cracks into the soil matrix usually leads to severely underestimated infiltration rates, too high predictions of water accumulating at or near the soil surface, overestimation of surface runoff, and, consequently, unrealistic descriptions of the soil water regime.

Soils generally contain two types of pores (Doležal and Kutílek 1972): (1) Micropores that form a relatively homogeneous system, depending mostly upon soil texture; and (2) macropores that can be divided into major groups. One group consists of relatively stable macropores created by plant roots and soil fauna. Such macropores are more or less independent of the soil water content. A second group consists of soil cracks whose dimensions are dependent upon the soil water content and on the soil mechanical properties. If the soil matrix reflects a bimodal porosity, micropores can be further subdivided into interpedal and intrapedal micropores (Kutílek and Nielsen 1994).

When modeling a soil containing relatively stable macropores, its saturated hydraulic conductivity K_s can be characterized by a lumped parameter to be estimated at the scale of a representative elementary volume of soil (e.g., using the Guelph permeameter) (Reynolds 1993). Soils containing drying cracks cannot be characterized in such a way as the cracks are relatively unstable. Their geometry changes with time depending upon the soil water content, and their hydraulic conductivity is extremely high as compared with the soil matrix K_s.

The importance of soil cracks, particularly for infiltration into fine-textured (clay) soils during rainfall or irrigation is widely recognized [e.g., Kutílek and Novák (1976) and Mitchell and van Genuchten (1993)]. Fig. 1 shows a typical crack net developed under a spring barley canopy on June 6, 1995, at the Trnava experimental site in southern Slovakia. The vol-

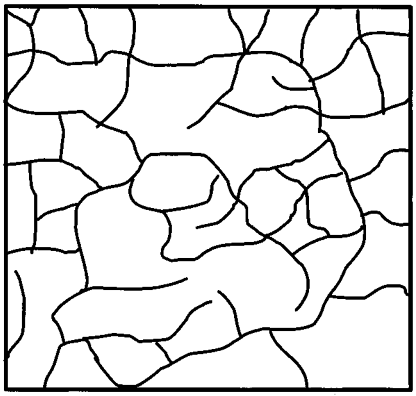

FIG. 1. System of Soil Cracks in 1-m Square Area of Soil Surface at Trnava Experimental Site in Southern Slovakia, June 6, 1995. A Real Crack Porosity at Soil Surface $P_c(0) = 0.046$ m^2/m^2 and the Specific Length of the Cracks $l_c = 11.1$ m/m^2

---

[1] Sr. Sci., Inst. of Hydro., Slovak Acad. of Sci., P.O. Box 94, Račianská 75, 830 08 Bratislava, Slovak Republic.

[2] Asst. Res., U.S. Salinity Lab., US Dept. of Agr., ARS, 450 West Big Springs Rd., Riverside, CA, 92507-4617.

[3] Res. Leader, U.S. Salinity Lab., US Dept. of Agr., ARS, 450 West Big Springs Rd., Riverside, CA.

Note. Discussion open until July 1, 2000. To extend the closing date one month, a written request must be filed with the ASCE Manager of Journals. The manuscript for this paper was submitted for review and possible publication on March 22, 1999. This paper is part of the ***Journal of Irrigation and Drainage Engineering***, Vol. 126, No. 1, January/February, 2000. ©ASCE, ISSN 0733-9437/00/0001-0041–0047/$8.00 + $.50 per page. Paper No. 20554.

ume of cracks under a 1-m^2 area of soil surface at the time of the measurement was about 0.005 m^3 (i.e., a water layer of 5 mm was needed to fully fill the crack system). The surface of the crack walls, again under a 1-m^2 area of the soil surface, was 12.1 m^2, which implies that the maximum potential infiltration surface is 12.1 times larger than the soil topographic surface. These numbers illustrate the potential importance of cracks in affecting the soil water regime of fine-textured, swelling soils.

A variety of models describing the movement of water and dissolved solutes in soils containing cracks have been developed, most of them based on schematic representations of the crack network (van Genuchten 1991; Ma and Selim 1998; van Genuchten and Sudicky 1999). Results obtained with these models are still relatively poor, in part because of conceptual weaknesses in the models, and in part because of difficulties in accurately estimating crack input parameters. Flow in structured porous media is frequently also described using dual-permeability models (Pruess and Wang 1987; Gerke and van Genuchten 1993a; Jarvis 1994, 1998). Approaches of this type assume that the soil consists of two regions, one associated with macropores (the crack network), and the other with the less-permeable matrix region. The difficulty in applying this approach to cracked soils is that flow in both regions is described using the Richards' equation, an assumption that is likely not valid for flow in large drying cracks. For example, the MACRO dual-permeability model of Jarvis (1994) uses the Richards' equation and the convection-dispersion equation to model soil water flow and solute transport in the matrix (soil micropores), whereas flow and transport in the macropores is described using a simplified capacitance-type approach. The exchange between matrix and macropore regions is simulated with an approximate quasi-empirical first-order rate expression (Jarvis 1994).

Another class of models uses the statistical properties of cracks (e.g., depth and width). This approach does not require detailed knowledge of the crack system and/or the spatial distribution of macropores (Slawinski et al. 1996; van Dam et al. 1997). For example, the SWIMv2.1 model (Verburg et al. 1996) assumes that water and solutes from runoff, after the infiltration capacity of the soil is exceeded and a critical depth of water is formed at the soil surface, can move directly to specified bypass depths. Downward bypass will not occur if the matrix absorbs all water through the soil surface. The latest version of the SWATRE model, SWAP (van Dam et al. 1997), also adds infiltrated water from cracks as a source term to Richards' equation. This model, however, assumes lateral infiltration from the cracks into the soil matrix to be constant in time, as long as water is present in the cracks, with the infiltration rate changing only as a function of the active crack area. The infiltration rate itself is calculated using Darcy's law.

In this study the FRACTURE submodel that quantitatively describes the infiltration of rain or irrigation water into an initially relatively dry, cracked, fine-textured soil is presented. Variably saturated flow in the soil matrix is described using the Richards' equation. Excess water at the soil surface that cannot infiltrate because of a low infiltration capacity is either removed by surface runoff, or allowed to fill the soil cracks from where it infiltrates laterally into the soil matrix. Infiltration from the soil cracks into the soil matrix is locally assumed to be horizontal and described using the Green-Ampt approach.

CONCEPTUAL MODEL

A schematic of the conceptual model forming the basis of the FRACTURE submodel is shown in Fig. 2. Precipitation or irrigation $q_0(t)$ falls on the soil surface and, as long as the soil surface is unsaturated, is equal to the actual infiltration rate $q(t)$. The model assumes that all precipitation falls directly on the soil surface. After the soil surface becomes saturated (at ponding time t_p), excess water is first used to form a surface layer, the maximum thickness of which is a function of the surface roughness. The soil surface is hence assumed to have a certain roughness that causes the detention of some water and prevents it from running off or flowing into cracks. Although the surface roughness can change with time due to impact of the kinetic energy of rain (Verburg et al. 1996), the roughness is considered to be constant with time. It is further assumed that surface runoff or flow into cracks can start only after the surface water layer reaches a critical thickness h_s. At that time water starts flowing into the cracks as long as the precipitation or irrigation rate is higher than the actual surface infiltration flux. When the applied surface flux becomes smaller than the actual infiltration rate, flow into cracks stops and water in the soil surface layer infiltrates directly into the soil until it is completely used.

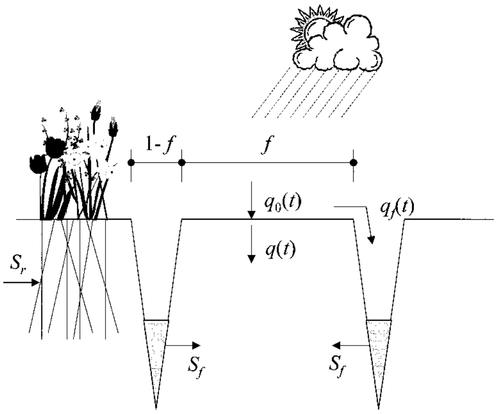

FIG. 2. Schematic of FRACTURE Submodel. Applied Surface Flux $q_0(t)$ Is Divided between Soil Surface Infiltration Rate $q(t)$ and Flow into Cracks $q_f(t)$. $S_f(z, t)$ Represents Horizontal Infiltration Rate from Cracks into Soil Matrix

The infiltration process can thus be divided into several stages:

1. Unsaturated infiltration when the soil surface is still unsaturated: $q(t) = q_0(t)$, $t_p < t$
2. The formation (or disappearance) of a surface layer of water after the soil surface becomes saturated: $q(t) < q_0(t)$ [or $q(t) > q_0(t)$]
3. Flow into cracks when the soil surface is saturated and the surface water layer has reached a certain critical height h_s: $q(t) < q_0(t)$
4. Runoff when cracks are either full or not considered: $q(t) < q_0(t)$
5. Horizontal infiltration from cracks into the soil matrix

It is further assumed that soil cracks during a certain precipitation event do not change their dimensions. The physical processes of crack formation and swelling, and particularly its quantification into mathematical models, still needs further investigation.

Horizontal infiltration of water into the soil matrix is considered only through crack surfaces that are in direct contact with water standing in the cracks. Hence, the model does not consider infiltration of film water flowing along crack walls. It is further assumed that excess surface water moves directly to the prevailing water level in the cracks.

MATHEMATICAL MODEL

The FRACTURE submodel described here is part of the HYDRUS-ET code (Šimůnek et al. 1997). The 1D Richards' equation is assumed to describe water flow in the soil matrix. Matrix and preferential flow are mutually linked using an extension of the Richards' equation as follows (Feddes et al. 1988):

$$\frac{\partial\theta}{\partial t} = \frac{\partial}{\partial z}\left[K(h, z)\left(\frac{\partial h}{\partial z} + 1\right)\right] - S_r(z) + S_f(z) \qquad (1)$$

where h = pressure head; θ = volumetric water content; t = time; z = vertical coordinate (positive upward); K = unsaturated hydraulic conductivity; $S_r(z)$ = sink term quantifying the volume of water extracted from soil by roots; and $S_f(z)$ = horizontal infiltration rate of water from the water-filled part of soil cracks into the soil matrix. This term is calculated using the Green-Ampt approach (Green and Ampt 1911)

$$S_f = \left(K_h(z)\,\frac{h_0 - h_f}{l_f}\right)A_c \qquad (2)$$

where K_h = hydraulic conductivity of the crack-matrix interface; h_0 = positive pressure head at the point of infiltration; h_f = pressure head at the wetting front at horizontal distance l_f away from the crack surface; and A_c = specific surface of the cracks. The hydrostatic pressure is used as the pressure head h_0 at nodes where lateral fracture flow occurs. The wetting front distance l_f can be calculated according to the Green-Ampt approach as follows:

$$l_f = \sqrt{2K_h\,\frac{h_0 - h_f}{\theta_s - \theta_i}\,t_f} \qquad (3)$$

where θ_i and θ_s = initial and saturated volumetric water contents, respectively; and t_f = time interval since the start of infiltration.

The Richards' equation for flow in the matrix is solved numerically subject to a set of initial and boundary conditions as summarized below.

Initial Condition

The initial condition is the result of hydrologic processes prior to the infiltration event and given by the soil water pressure head profile

$$h(z) = h_i(z) \quad \text{for} \quad t = t_0 \qquad (4)$$

where h_i = initial pressure head; and t_0 = initial time.

Upper Boundary Conditions

The upper boundary condition during an infiltration event depends on the actual status of the soil surface. Three different boundary conditions at the soil surface are used to characterize different stages of the infiltration process.

Stage 1. When the soil surface is unsaturated a flux boundary condition is used

$$-K\left(\frac{\partial h}{\partial z} + 1\right) = q_0(t) \quad \text{for} \quad h < 0 \qquad (5)$$

where q_0 = applied surface flux (i.e., the difference between evaporation and precipitation/irrigation). Because of the orientation of the z-coordinate, q_0 is positive for evaporation and negative for infiltration. Although HYDRUS-ET considers evaporation from the soil surface (not across crack walls), evaporation is negligibly small for a timescale used in the example given below.

Stage 2. When the surface is saturated and the surface water layer is either being formed or depleted, a ''surface reservoir'' boundary condition is used (Mls 1982):

$$-K_s\left(\frac{\partial h}{\partial z} + 1\right) = q_0(t) - \frac{dh}{dt} \quad \text{for} \quad 0 < h < h_s \qquad (6)$$

where K_s = saturated hydraulic conductivity of the soil matrix; and h_s the critical thickness of the water layer on the soil surface when surface runoff is initiated, or when water starts flowing into cracks. The surface reservoir boundary condition [(6)] permits a water layer to either build up at the soil surface, or be used up for infiltration. The left-hand side represents the actual infiltration rate into the soil profile through the soil surface. The first term on the right side, q_0, represents the applied surface flux, and the second term is the change in the thickness of the water layer at the soil surface.

Boundary condition (6) applies when the soil surface is already saturated, but the value of the critical head h_s is not yet reached. During this time the surface water layer is being formed, depending upon the actual infiltration rate and the applied surface flux. Boundary condition (6) is also used after the precipitation/irrigation event has ended (or when the precipitation/irrigation rate is or has become lower than the sum of the actual infiltration rate and evaporation), and surface water is being used for infiltration and evaporation.

Stage 3. When the surface layer reaches the critical thickness h_s, a boundary condition is used that either specifies the flow rate into the soil cracks, or the rate of runoff. In that case

$$h = h_s \quad \text{for} \quad |q_0(t)| > |q(t)| \qquad (7)$$

where q = actual infiltration rate. Flow into the cracks, or surface runoff q_f, is calculated as follows:

$$q_f(t) = q_0(t) + K_s\left(\frac{\partial h}{\partial z} + 1\right) \qquad (8)$$

Boundary condition (7) is used when the surface layer reaches the critical thickness h_s; the applied surface flux q_0 is still larger that the actual infiltration rate q; and all excess water either flows into cracks or is removed by surface runoff.

The amount of water in the cracks V_f is calculated as

$$V_f = \left(\int_t q_f(t)\,dt - \int_t q_{fs}(t)\,dt\right) \qquad (9)$$

where q_{fs} = water flux rate from the cracks into the soil matrix.

Lower Boundary Conditions

A variety of boundary conditions, the same as those used in the HYDRUS-ET model (Šimůnek et al. 1997), can be prescribed at the lower boundary. The conditions include constant or variable pressure heads or fluxes, seepage faces, and deep or free drainage conditions.

Input Data

In addition to parameters needed by HYDRUS-ET, the coupled HYDRUS-ET FRACTURE model needs parameters characterizing flow into and from the soil cracks. First, the model requires the crack porosity P_c as a function of the soil gravimetric water content w, $P_c(w)$ (i.e., a soil shrinkage characteristic curve) (Mitchell 1992). This relationship is a soil characteristic and can be estimated in the laboratory on undisturbed soil samples. As the soil sample slowly dries, changes in its height and diameter are measured simultaneously with changing soil water content w. The shrinkage curve $P_c(w)$ can be easily estimated assuming that the soil sample deformation is equal to the soil crack porosity P_c (Novák, unpublished paper, 1999). The crack porosity profile $P_c(z)$ can then be estimated using the measured or calculated soil water content profile $w(z)$ and the relationship $P_c(w)$. Second, the specific length of cracks l_c per unit soil surface area is needed. This length is assumed to be constant over the depth of crack formation (i.e, constant between the soil surface and the bottom part of the cracks). The length can be estimated in the field by direct measurement or by image analysis of the site under consideration.

MODEL APPLICATION

An example is now presented to illustrate differences between the traditional approach of calculating infiltration and our method for simulating infiltration into a soil containing drying cracks. The model was applied to a fine-textured (clay) soil from the Trnava area of southern Slovakia. The hydraulic parameters of the soil are as follows: residual soil water content $\theta_r = 0.03$, saturated soil water content $\theta_s = 0.407$, parameter $\alpha = 0.774\ \text{cm}^{-1}$, parameter $n = 1.235$, and saturated hydraulic conductivity of the soil matrix $K_s = 5$ cm/day (van Genuchten 1980). The soil cracks were estimated in the field to have a specific length of the soil cracks $l_c = 0.046\ \text{m/m}^2$. The shrinkage curve $P_c(w)$ (i.e., the relationship between crack porosity and the soil water content) was measured in the laboratory. The $P_c(w)$ data, and its linear approximation for the upper soil layer at the Trnava experimental site, are shown in Fig. 3. The linear approximation is given by (Novák, unpublished paper, 1999)

$$P_c = -a_f w + P_{c0} \tag{10}$$

where a_f = slope; and P_{c0} = maximum crack porosity corresponding to a zero soil water content w.

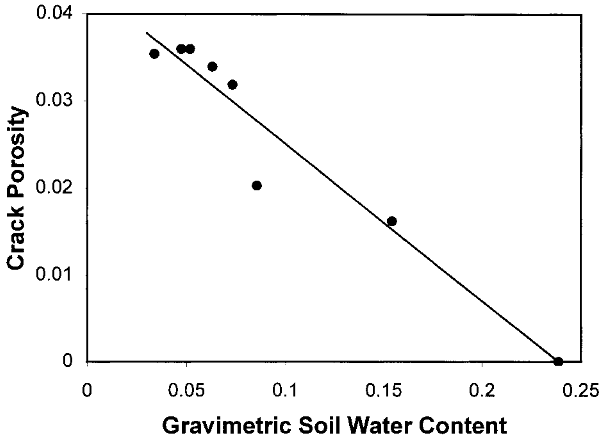

FIG. 3. Crack Porosity P_c versus Gravimetric Soil Water Content w for Trnava Experimental Site in Southern Slovakia

Horizontal infiltration from the cracks into the soil matrix is simulated using the hydraulic conductivity of the crack-matrix interface K_h [see (2) and (3)], which is related to the matrix saturated hydraulic conductivity K_s as follows:

$$K_h = r_k K_s \tag{11}$$

where r_k = reduction factor accounting for hydraulic resistances across the crack-soil matrix interface. Thomas et al. (1992) conducted experiments showing that due to coatings the hydraulic conductivity of the fracture-matrix interface of fracture rock may be much smaller than the matrix conductivity. Gerke and van Genuchten (1993b) and van Genuchten and Sudicky (1999) reviewed experimental evidence indicating that the interface hydraulic conductivity can be smaller by several orders of magnitude than the conductivity of the matrix interior. They reasoned that this is probably due to the changed physical and chemical properties of the interface as a result of repeated opening and closing of fractures and of coating of the interface by relicts of roots and other organic matter. Techniques for directly measuring the hydraulic conductivity of fracture-matrix interfaces (or of soil macropore walls) are only recently being perfected (Gerke and Köhne 1999). Field observations have shown that soil cracks form along the same internal soil surfaces that represent areas of minimum mechanical strength.

The following crack characteristics were used in our numerical experimental: $z_c = 40$ cm, $a_f = 0.178$, $P_{c0} = 0.429$, and $r_k = 0.1$, where z_c is the depth of soil cracks. Simulations were carried out assuming an irrigation rate q_0 of 25 cm/day for a period of $t = 2$ h. Surface runoff, or flow into cracks, was assumed to start when the thickness of the soil surface water layer reached a critical value h_s of 0.1 cm.

RESULTS AND DISCUSSION

Fig. 4 shows calculated soil water content profiles for different times during infiltration into the soil for three scenarios: (1) A soil without crack with water accumulating at the soil surface [Fig. 4(a)]; (2) a soil without cracks but with surface runoff [Fig. 4(b)]; and (3) a soil with cracks [Fig. 4(c)]. The figure shows a distinct area above the maximum crack depth (40 cm) through which water and solutes infiltrate into the soil profile when crack infiltration is being considered (Scenario 3).

The infiltration rates corresponding to the different scenarios described above are shown in Fig. 5. The vertical infiltration rate with surface runoff present (Scenario 2) is the same as the infiltration rate through the soil surface of the cracked soil

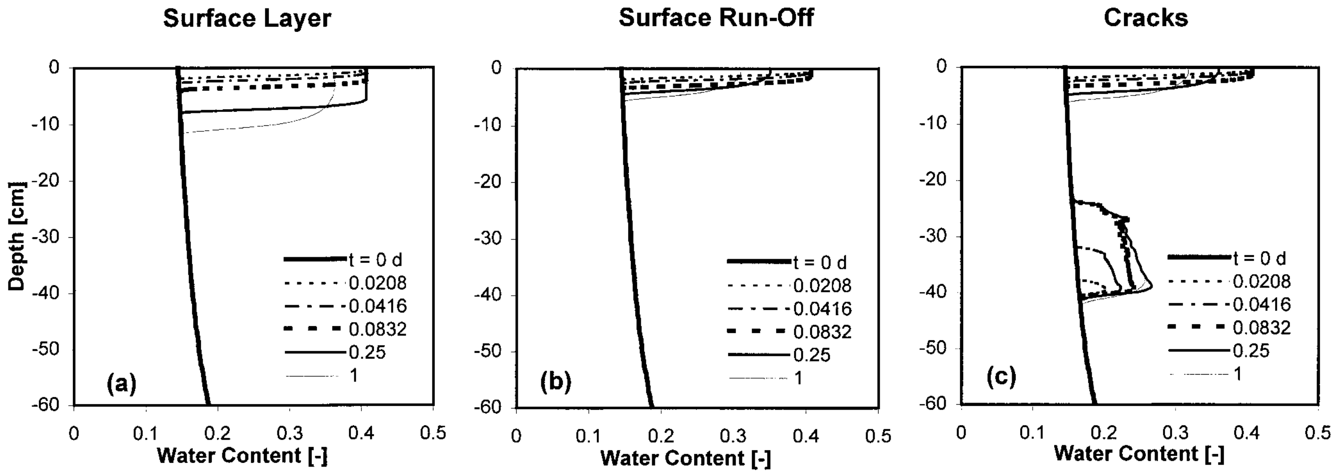

FIG. 4. Soil Water Content Profiles during Infiltration into Soil: (a) without Cracks with Water Accumulating on Soil Surface; (b) without Cracks with Surface Runoff; (c) with Cracks

(Scenario 3). This rate (Curve 3) is slightly lower than the infiltration rate into the soil when water is allowed to accumulate on top of the soil surface (Scenario 1; no surface runoff, and no cracks) (Curve 2, Fig. 5). The instantaneous infiltration rate, as well as the cumulative infiltration rate, into the soil is higher when ponding at the soil surface is allowed above the critical surface layer (Scenario 1) as compared to Scenarios 2 and 3 where the surface water layer cannot exceed the critical thickness h_s. This is caused by water accumulating on top of the soil surface that increases the pressure head and, consequently, the pressure gradient across the soil surface. Ponded infiltration will continue after the end of the precipitation event until all water accumulated on the soil surface has infiltrated (Curve 2, Fig. 5).

The important differences between the various infiltration events involving different boundary conditions (i.e., with and without a surface layer, runoff, or cracks) are further illustrated in Fig. 6, which shows plots of the cumulative infiltration rate of water for all simulated cases. Depending upon the scenarios involved, applied (rain or irrigation) water exceeding the infiltration capacity of the soil is either temporarily stored in a surface layer or in the soil cracks (Fig. 7), or is lost due to surface runoff.

The ponded water layer on the soil surface for the first simulation (Scenario 1) starts forming at 0.01 day, reaches a maximum of about 1.3 cm at the end of the irrigation event (0.1 day), and is fully depleted at about 0.305 day. Fig. 7 presents the amount of water stored in the cracks for the third simulation (Scenario 3). Although water flowing into the cracks (Curve 5, Fig. 5) can significantly increase the total actual

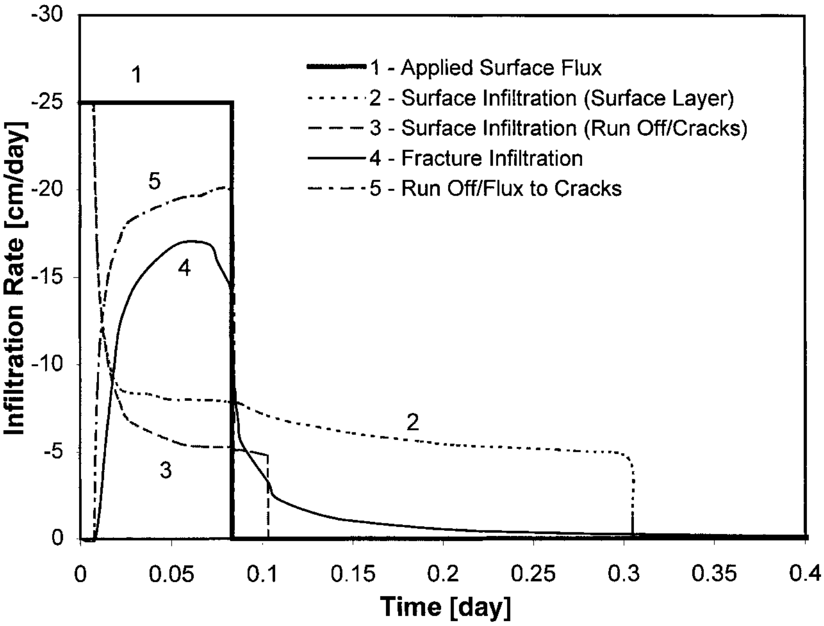

FIG. 5. Infiltration Rates versus Time for Three Scenarios Considered in This Study: Curve 1, Irrigation Rate $q_0(t)$; Curve 2, Infiltration $q(t)$ into Soil without Cracks with Water Accumulating on Soil Surface; Curve 3, Infiltration $q(t)$ through Soil Surface into Soil with Surface Runoff (with or without Cracks Present); Curve 4, Infiltration $q_f(t)$ from Cracks into Soil Matrix; Curve 5, Flow into Cracks $[q_0(t) - q(t)]$

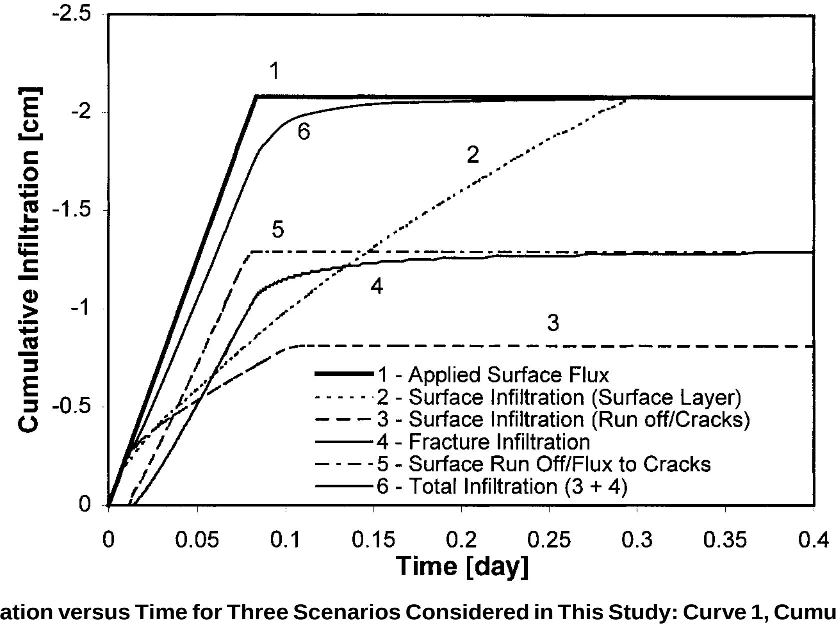

FIG. 6. Cumulative Infiltration versus Time for Three Scenarios Considered in This Study: Curve 1, Cumulative Irrigation Rate; Curve 2, Cumulative Infiltration into Soil without Cracks with Water Accumulating on Soil Surface; Curve 3, Cumulative Infiltration through Soil Surface into Soil with Surface Runoff (with or without Cracks Present); Curve 4, Cumulative Infiltration from Cracks into Soil Matrix; Curve 5, Cumulative Flow into Cracks; Curve 6, Total Cumulative Infiltration into Soil Matrix for Soil with Cracks

infiltration rate into the soil matrix, applied water accumulated on top of the soil surface prolongs the infiltration process until after the end of precipitation/irrigation (Curve 2, Fig. 5). Notice that the total cumulative infiltration rate into the cracked soil [i.e., infiltration through both the soil surface and the crack walls (Curve 6 in Fig. 6)] most closely resembles the applied surface flux (Curve 1). Thus, the cracks can significantly increase the total infiltration capacity of the soil in comparison with other simulated scenarios when the applied irrigation rate is higher than the saturated hydraulic conductivity.

The unique contribution of cracks to the infiltration process is clearly visible in Figs. 5 and 6. Infiltration via the cracks (Curve 4) is initially zero and remains so until after 0.01 day when ponding develops and water flows into the cracks. This delay includes the time interval during which the thin water layer developed on the soil surface. Only when the water layer reached the critical thickness h_s did water start to flow into the cracks and from there infiltrated laterally into the soil matrix. The infiltration rate from the cracks subsequently increased quickly as more water flowed into the cracks and a larger surface area of the cracks became involved in the infiltration process. After reaching a maximum, the infiltration rate from the cracks started to decrease before the end of the precipitation/irrigation event, mostly because of the decreasing rate of horizontal infiltration (in response to decreasing lateral pressure gradients). However, the water level as well as the water volume in the crack kept increasing up to the end of precipitation (Fig. 7). The highest infiltration rates from the cracks into the soil occurred across crack walls that just became active for infiltration, due to locally high gradients in the soil water pressure head associated with infiltration into relatively dry soil. As shown in Fig. 8, infiltration rates from the crack

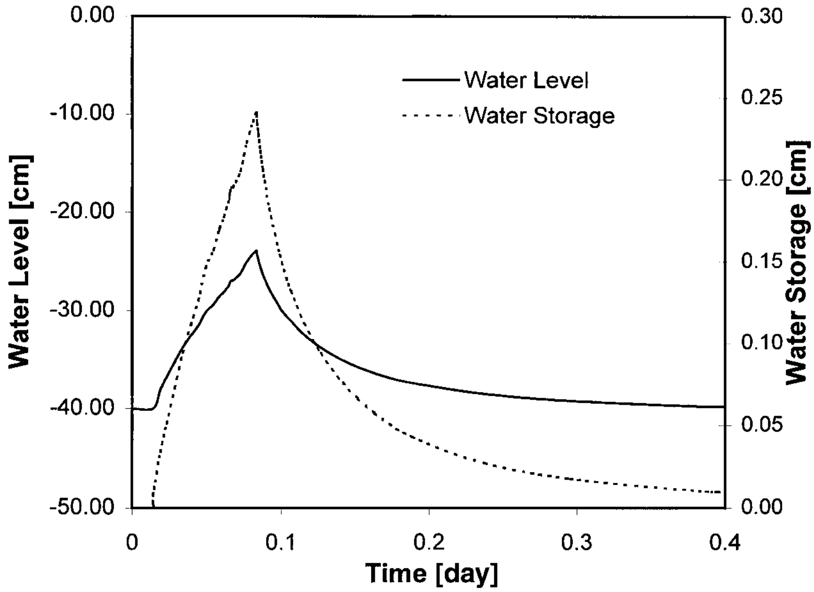

FIG. 7. Water Level (Depth below Soil Surface) and Amount of Water in Cracks during Infiltration

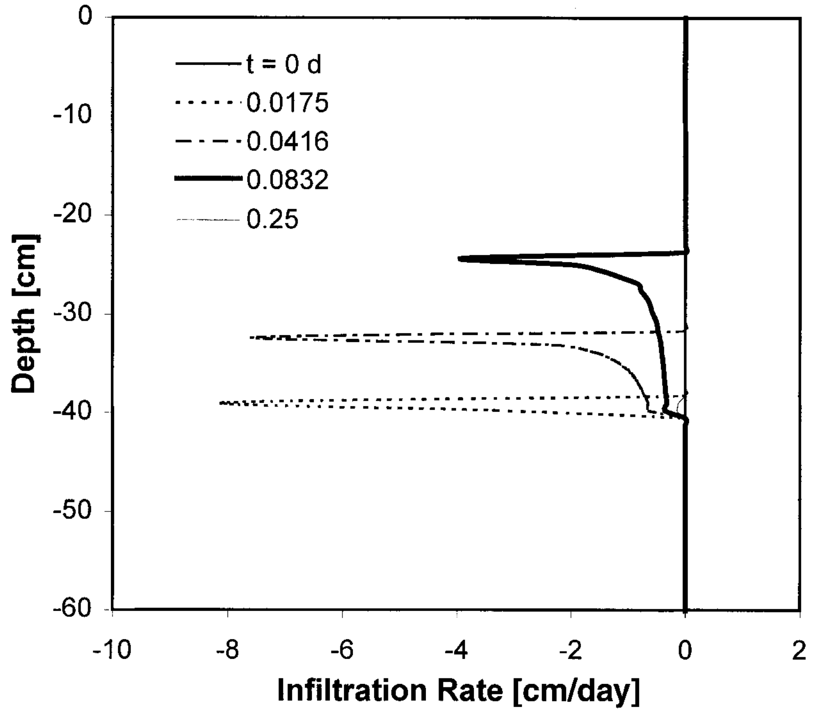

FIG. 8. Local Infiltration Rates through Crack Walls

to the soil slowly decrease as the infiltration process proceeds. Notice also that, as expected, the infiltration maximum slowly shifts toward the soil surface where relatively dry soil is continually being encountered as the water level rises.

CONCLUSIONS

The example presented in the paper demonstrates the importance of soil cracks in determining rates of infiltration into a soil during irrigation. In our example the infiltration capacity of the soil without cracks is less than half (34%) of the infiltration capacity of the soil with cracks. This corresponds very closely with values measured by Mitchell and van Genuchten (1993) for two fallow irrigations (36.1 and 35.4%) of a cracked soil in a large weighing lysimeter. A comparison with the more traditional approach involving only surface infiltration indicates important differences in the soil water content distribution during an irrigation event. An extension of the classical Richard's equation approach to include crack infiltration can lead to significantly improved predictions of the water regime of swelling clay soils.

APPENDIX I. REFERENCES

Doležal, F., and Kutílek, M. (1972). ''Flow of water in swelling soils.'' *Proc., 2nd Symp. Fundamentals of Transport Phenomena in Porous Media*, IAHR-ISSS, Vol. 1, 292–305.

Feddes, R. A., Kabát, P., van Bakel, J., Bronswijk, J. J. B., and Halbertsma, J. (1988). ''Modeling soil water dynamics in the unsaturated zone—state of art.'' *J. Hydro.*, Amsterdam, 100, 69–111.

Gerke, H. H., and Köhne, J. M. (1999). ''Impact of clayey coatings on hydraulic properties of soil aggregates.'' *Geophys. Res. Abstracts*, 1(2), 324.

Gerke, H. H., and van Genuchten, M. Th. (1993a). ''A dual-porosity model for simulating the preferential movement of water and solutes in structured porous media.'' *Water Resour. Res.*, 29(2), 305–319.

Gerke, H. H., and van Genuchten, M. Th. (1993b). ''Evaluation of a first-order water transfer term for variably saturated dual-porosity flow models.'' *Water Resour. Res.*, 29(4), 1225–1238.

Green, W. H., and Ampt, G. A. (1911). ''Studies on soil physics: 1. Flow of air and water through soils.'' *J. Agr. Sci.*, 4, 1–24.

Jarvis, N. J. (1994). ''The MACRO model (version 3.1)—Technical description and sample simulations.'' *Rep. and Dissertations 19*, Dept. of Soil Sci., Swedish University of Agricultural Sciences, Uppsala, Sweden.

Jarvis, N. J. (1998). ''Modeling the impact of preferential flow on nonpoint source pollution.'' *Physical nonequilibrium in soils: modeling and application*, J. M. Selim and L. Ma, eds., Ann Arbor Press, Chelsea, Mich., 195–221.

Kutílek, M., and Nielsen, D. R. (1994). *Soil hydrology.* Catena Verlag, Cremlingen, Germany.

Kutílek, M., and Novák, V. (1976). ''The influence of soil cracks upon infiltration and ponding time.'' *Proc., Symp. Water and Heavy Soils*, M. Kutílek and J. Šutor, eds., Vol. 1, Institute of Hydrology, Slovak Academy of Sciences, Bratislava, Slovakia, 26–134.

Ma, L., and Selim, H. M. (1998). ''Coupling of retention approaches to physical nonequilibrium models.'' *Physical nonequilibrium in soils: Modeling and application*, J. M. Selim and L. Ma, eds., Ann Arbor Press, Chelsea, Mich., 83–115.

Mitchell, A. R. (1992). ''Shrinkage terminology: Escape from 'normalcy'.'' *Soil Sci. Soc. Am. J.*, 56, 993–994.

Mitchell, A. R., and van Genuchten, M. Th. (1993). ''Flood irrigation of a cracked soil.'' *Soil Sci. Soc. Am. J.*, 57, 490–497.

Mls, J. (1982). ''Formation and solution of fundamental problems of vertical infiltration.'' *Vodohosp. Čas*, 30, 304–313 (in Czech).

Pruess, K., and Wang, J. S. Y. (1986). ''Numerical modeling of isothermal and nonisothermal flow in unsaturated-saturated fractured rock—a review.'' *Flow and transport through unsaturated fracture rock*, D. D. Evans and T. J. Nicholson, eds., American Geophysics Union, Washington, D.C., 11–22.

Reynolds, W. D. (1993). ''Unsaturated hydraulic conductivity: Field measurement.'' *Soil sampling and methods of analysis*, M. R. Carter, ed., Lewis, Boca Raton, Fla., 633–644.

Šimůnek, J., Huang, K., Šejna, M., van Genuchten, M. Th., Majerčák, J., Novák, V., and Šutor, J. (1997). *The HYDRUS-ET software package for simulating the one-dimensional movement of water, heat and multiple solutes in variably—Saturated media. Version 1.1.* Institute of Hydrology, Slovak Academy of Sciences, Bratislava, Slovakia.

Slawinski, C., Sobczuk, H. A., and Walczak, R. T. (1996). ''Submodel of bypass flow in cracking soil. Part 1. Theory.'' *Int. Agrophysics*, Lublin, Poland, 10, 189–196.

Thoma, S. G., Gallegos, D. P., and Smith, D. M. (1992). ''Impact of fracture coating on fracture/matrix flow interaction in unsaturated porous media.'' *Water Resour. Res.*, 28, 1357–1367.

van Dam, J. C., et al. (1997). ''Theory of SWAP, version 2.0. Simulation of water flow, solute transport and plant growth in the soil-water-atmosphere-plant environment.'' *Rep. 71, Tech. Document 45*, Dept. Water Resources, Wageningen Agricultural University, The Netherlands, Dienst Landbouwkundig Onderzoek (Agricultural Research Department) Winand Staring Centre, Wageningen.

van Genuchten, M. Th. (1980). ''A closed-form equation for predicting the hydraulic conductivity of unsaturated soils.'' *Soil Sci. Soc. Am. Proc.*, 44, 892–898.

van Genuchten, M. Th. (1991). ''Progress and opportunities in hydrologic research.'' *Rev. of Geophys.*, Supplement, 189–192.

van Genuchten, M. Th., and Sudicky, E. A. (1999). ''Recent advances in vadose zone flow and transport modeling.'' *Vadose zone hydrology: cutting across disciplines*, M. B. Parlange and J. W. Hopmans, eds., Oxford University Press, New York, 155–193.

Verburg, K., Ross, P. J., and Bristow, K. L. (1996). ''SWIMv2.1 user manual.'' *Divisional Rep. No. 130*, Commonwealth Scientific and Industrial Research Organization, Australia.

APPENDIX II. NOTATION

The following symbols are used in this paper:

A_c = specific surface of cracks (L^2 L^{-3});
a_f = slope of $P_c(w)$ function (nondimensional);
h = pressure head (L);
h_f = pressure head (negative) at wetting front at distance l_f away from crack surface (L);
h_i = initial pressure head (L):
h_s = critical head (L) (i.e., thickness of water layer at soil surface when surface runoff is initiated) or when water starts flowing into soil cracks (L);
h_0 = positive pressure head at point of infiltration (L);
K = unsaturated hydraulic conductivity (L T^{-1});
K_h = hydraulic conductivity of crack-matrix interface (L T^{-1});
K_s = saturated hydraulic conductivity of soil matrix (L T^{-1});
l_c = specific length of cracks per unit soil surface area (L L^{-2});
l_f = distance of wetting front from infiltration surface (L);
n = parameter of van Genuchten's equation (1980) (nondimensional);
P_c = crack porosity (L^3 L^{-3});
P_{c0} = maximum crack porosity corresponding to zero soil water content w (L^3 L^{-3});
q = actual infiltration rate (L^3 L^{-2} T^{-1});
q_f = flow into soil cracks or surface runoff (L^3 L^{-2} T^{-1});
q_{fs} = water flux rate from cracks into soil matrix (L^3 L^{-2} T^{-1});
q_0 = potential infiltration rate (L^3 L^{-2} T^{-1});
r_k = reduction factor for saturated hydraulic conductivity of crack-soil matrix interface (nondimensional);
S_f = horizontal infiltration rate of water from cracks into soil matrix (L^3 L^{-3} T^{-1});
S_r = sink term (L^3 L^{-3} T^{-1}) quantifying volume of water extracted from soil by roots (root extraction term);
t = time (T);
t_f = time interval since the start of infiltration (T);
t_p = ponding time (T);
t_0 = initial time (T);
V_f = volume of water in cracks (L^3 L^{-2}) under unit square area of soil surface;
w = soil gravimetric water content (M^3 M^{-3});
z = vertical coordinate (L) (positive upward);
α = parameter of van Genuchten's equation (1980) (L^{-1});
θ = volumetric water content (L^3 L^{-3});
θ_i = initial volumetric water contents (L^3 L^{-3});
θ_r = residual soil water content (L^3 L^{-3}); and
θ_s = saturated soil water content (L^3 L^{-3}).